Rotor Current Oriented Control Method of DFIG-DC System Without Stator Side Sensors

Wu, Chao; Cheng, Peng; Nian, Heng; Blaabjerg, Frede

Published in:
I E E E Transactions on Industrial Electronics

DOI (link to publication from Publisher):
10.1109/TIE.2019.2956415

Publication date:
2020

Document Version
Accepted author manuscript, peer reviewed version

This article has been accepted for publication in a future issue of this journal, but has not been fully edited. Content may change prior to final publication. Citation information: DOI 10.1109/TIE.2019.2956415, IEEE Transactions on Industrial Electronics

Rotor Current Oriented Control Method of DFIG-DC System Without Stator Side Sensors

Chao Wu, Peng Cheng, Heng Nian, *Senior Member, IEEE* and Frede Blaabjerg, *Fellow, IEEE*

***Abstract*—This letter proposes a novel stator power and frequency control method of DFIG-DC system, which is based on rotor current orientation and avoids using stator side sensors. By means of establishing the relationship of the rotor current vector, stator active power and stator frequency, the stator active power can be controlled by the angle between rotor current vector and stator voltage vector. The stator frequency can be controlled by the magnitude of rotor current magnitude. The stator active power is calculated by dc voltage and dc current at stator side. In this way, the stator voltage and current sensors can both be eliminated. Furthermore, the stator frequency and orientation angle are acquired by the power control loop, which avoids using voltage model or current model. In this way, parameter dependency and dc sampling uncertainties can both be eliminated. Finally, experiments based on a 1 kW DFIG-DC setup is carried out to verify the proposed method.**

***Index Terms*— Doubly-fed induction generator (DFIG), rotor current orientation, less sensor, power control**

I. Introduction

With the rapid development of dc transmission and dc micro grid, new topologies and control strategies of DFIG connected to dc grid have gained much attention [1]-[3]. The DFIG-DC system topology, in which only one full-controlled converter is needed, has been widely studied due to its simple structure and reduced cost. However, the vector control strategies based on conventional phase locked loop (PLL) is not applicable due to the diode bridge on the stator side [4]. Furthermore, the stator frequency needs to be controlled additionally since there is no ac grid on the stator side of DFIG. Thus, the two main control objectives of DFIG-DC system are the stator frequency and power (or torque) control to achieve the MPPT of wind turbine.

In [5]-[7], the decoupling control of stator frequency and torque is achieved by stator flux oriented control based on stator voltage model. The stator frequency is directly obtained by the derivative of stator flux angle which is highly dependent on parameters and the dc sampling offset of stator voltage may deteriorate the stator flux angle. In order to avoid the calculating process of stator frequency and stator flux angle, a stator flux PLL based on current model is proposed to acquire stator frequency and achieve stator flux oriented control [8]-[10]. However, all these control methods are based on stator voltage or stator current sensors, which are indispensable for control. In [11], the stator current is calculated based on rotor current and dc voltage for eliminating the stator side sensors, which is highly dependent on DFIG parameters.

In this letter, in order to avoid the stator voltage and current sensors, a novel stator frequency and power control method is proposed based on only regulating the rotor current vector. The relationship between angle of rotor current vector and stator power is revealed. Based on the relationship between rotor current magnitude and stator frequency, the stator frequency can be directly controlled through the magnitude of the rotor current vector. The advantages of this rotor current oriented control method can be concluded as:

1. Since the stator frequency is directly generated by the stator active power control loop, the voltage model or current model which is used to obtain the orientation angle can be avoided. Thus, the stator voltage and current sensors can both be eliminated.

2. The problem of parameter dependency and dc sampling offset can be avoided by using this method.

II. System Layout and Mathematical Model

The DFIG-DC system topology can be seen as Fig.1. When the diode rectifier is conducting, the steady state equivalent circuit of DFIG connected to diode bridge can be shown in Fig.2. The rotor side converter (RSC) and rotor side can be equivalent as a current source which is expressed as $\boldsymbol{I}_r$, $\boldsymbol{I}_s$ and $\boldsymbol{I}_m$ represent the stator and exciting current. $\boldsymbol{U}_s$ and $\boldsymbol{E}_m$ represent the stator voltage and air gap voltage, L_m and $L_{s\sigma}$ represent the mutual inductance and stator leakage inductance, R_s represents the stator resistance.

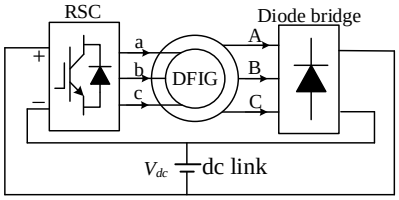

Fig. 1. DFIG connected to a DC Link through a diode rectifier.

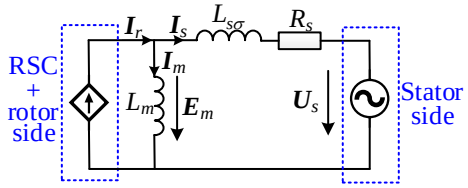

Fig. 2. Steady-state equivalent circuit for the DFIG-DC system.

In this letter, only the stator frequency and average stator power are considered while the harmonics in voltages and currents are both ignored. When the diode bridge is working in continuous conduction mode, the magnitude of the stator

This article has been accepted for publication in a future issue of this journal, but has not been fully edited. Content may change prior to final publication. Citation information: DOI 10.1109/TIE.2019.2956415, IEEE Transactions on Industrial Electronics

fundamental voltage can be expressed as,

$$|\boldsymbol{U}_s| = \frac{2}{\pi} V_{dc} \tag{1}$$

As it can be seen from (1), the magnitude of stator fundamental voltage is constant, which can be expressed by the product of stator frequency and stator flux. This characteristic can be used for controlling the stator frequency through the magnitude of rotor current vector.

Since the stator resistance can be ignored compared with stator leakage inductance, the air gap voltage can be simplified as,

$$\boldsymbol{E}_m = j\omega_s L_m \boldsymbol{I}_m = \boldsymbol{U}_s + j\omega_s L_{s\sigma} \boldsymbol{I}_s \tag{2}$$

where ω_s is the stator frequency which is also the rotating speed of rotor current vector.

Since the stator current is the same phase with stator voltage [8], the stator power can be calculated as,

$$P_s = \mathrm{Re}\left(\boldsymbol{U}_s \boldsymbol{I}_s\right) = \frac{L_m}{L_s} |\boldsymbol{U}_s| |\boldsymbol{I}_r| \cos\delta \tag{3}$$

where δ is the angle between rotor current and stator voltage, L_s is the stator inductance which is the sum of L_m and $L_{s\sigma}$.

As can be seen from (3), the stator power can be regulated through controlling angle δ.

According to the equivalent circuit in Fig. 2, the magnitude of stator flux can be expressed as,

$$|\boldsymbol{\psi}_s| \approx |\boldsymbol{\psi}_m| = L_m |\boldsymbol{I}_m| = L_m |\boldsymbol{I}_r| \sin\delta \tag{4}$$

From (4), it can be seen that the magnitude of stator flux is proportional to the magnitude of rotor current, which indicates that the magnitude of rotor current can be used for regulating magnitude of stator flux.

III. Control Strategy

The RSC control scheme for the power and stator frequency is shown as Fig. 3, the dc voltage is sampled as V_{dc} and the dc current at stator side is sampled as I_{dcs}, the rotor currents and rotor position are sampled for the RSC control. The control scheme can be divided into three parts: the stator active power control, stator frequency control and rotor current control. The power control loop is used for generating the stator frequency and the orientation angle, the stator frequency control is applied for generating the rotor current reference for controlling stator frequency, the rotor current control is the conventional inner current control loop. Through the proposed power and stator frequency control method, the stator voltage and current sensors can both be eliminated, which will be elaborated further in detail.

A. Output power Control

The stator active power can be calculated by the dc voltage and dc current at the stator side as,

$$P_s = V_{dc} \cdot I_{dcs} \tag{5}$$

As it can be seen from (3), the stator power will increase with the decrease of angle δ. The angle δ is the integral of rotating speed deviation between the rotor current vector and stator voltage vector. The angle δ will decrease with the increase of stator frequency, Thus, the stator frequency can be generated by the power control loop as,

$$\omega_s = \frac{k_{pp} s + k_{ip}}{s} \left(P_s^* - P_s\right) \tag{6}$$

where k_{pp} and k_{ip} are the proportional gain and integral gain of the power loop PI controller ($\mathrm{PI_p}$).

The orientation angle is the integral of stator frequency which can be expressed as,

$$\theta_s = \frac{1}{s} \omega_s \tag{7}$$

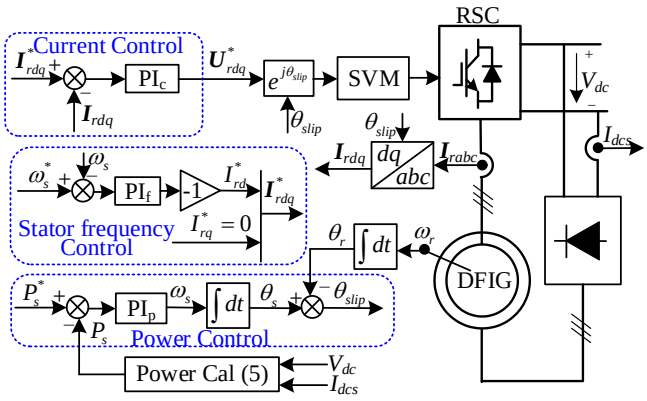

Fig. 3. RSC control scheme for power and frequency regulation of DFIG-DC system.

B. Stator frequency control

The q-axis rotor current is controlled to zero to achieve rotor current oriented control. Thus, the reference of q-axis rotor current is zero, which can be seen in Fig. 3. In this way, the magnitude of rotor current vector is equal to the d-axis rotor current. According to (4), the relationship between d-axis rotor current and stator frequency can be expressed as,

$$\omega_s = \frac{|\boldsymbol{U}_s|}{L_m I_{rd} \sin\delta} \tag{8}$$

As it can be seen from (8), the stator frequency is inverse ratio with d-axis rotor current. Combining (1) and (8), the d-axis rotor current can be used for controlling the stator frequency. Thus, the reference of d-axis rotor current can be given as,

$$I_{rd}^* = -\frac{k_{pf} s + k_{if}}{s} \left(\omega_s^* - \omega_s\right) \tag{9}$$

where k_{pf} and k_{if} are the proportional gain and integral gain of the stator frequency PI controller ($\mathrm{PI_f}$).

IV. Small Signal Analysis

In this section, the parameter design and stability analysis of the stator power and stator frequency control loop are presented through the small signal analysis. According to the stator power expression in (3), the relationship between stator power as well as the angle and magnitude of rotor current can be expressed by the partial differential as,

$$\frac{\partial P_s}{\partial \delta} = \frac{L_m}{L_s} |\boldsymbol{U}_s| |\boldsymbol{I}_{r0}| \left(-\sin\delta\right) \tag{10}$$

This article has been accepted for publication in a future issue of this journal, but has not been fully edited. Content may change prior to final publication. Citation information: DOI 10.1109/TIE.2019.2956415, IEEE Transactions on Industrial Electronics

$$\frac{\partial P_s}{\partial |\boldsymbol{I}_r|} = \frac{L_m}{L_s}|\boldsymbol{U}_s|\cos\delta \tag{11}$$

Since the relationship between stator power and rotor current vector is non-linear, a small signal model is deduced for the parameter design and stability analysis. Assuming that the steady state working point is P_{s0}, δ_0, $\boldsymbol{I}_{r0}$, the small signal of the power can be expressed as,

$$\Delta P_s = \frac{L_m}{L_s}|\boldsymbol{U}_s||\boldsymbol{I}_{r0}|(-\sin\delta_0)\Delta\delta + \frac{L_m}{L_s}|\boldsymbol{U}_s|\cos\delta_0\Delta|\boldsymbol{I}_r| \tag{12}$$

The relationship between the stator frequency and angle of rotor current vector can be expressed as,

$$\Delta\delta = -\frac{\omega_{base}}{s}\Delta\omega_s \tag{13}$$

where ω_{base} is equal to 100π rad/s.

As can be seen from Fig. 3, it contains three PI controllers in the control scheme, which can be divided as the stator power PI controller, stator frequency PI controller and rotor current PI controller (PI_c). The design procedure is first the inner loop and then the outer loop.

The design of rotor current PI controller is the same as conventional rotor current loop design which can be seen in [12]. The parameters of current PI controller are always designed based on the DFIG plant and the desired bandwidth. The DFIG plant can be modeled as an inertia plant shown in Fig. 4. The bandwidth of rotor current control loop is designed as 100 Hz. Meanwhile, the zero of the PI controller is designed to counteract the pole of the control plant for the sake of the constant −20 dB/dec before the crossover frequency [12].

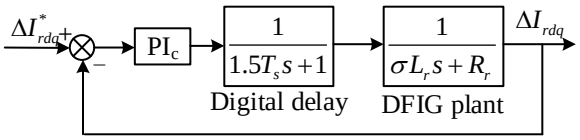

Fig. 4. Block diagram of rotor current control loop.

The rotor current control loop can be shown in Fig. 4. The parameters of DFIG is shown as Table I, R_r is equal to 0.88Ω, leakage coefficient σ is equal to 0.12, L_r is equal to 93.1 mH. The digital delay block represents the sampling and PWM delay, and the T_s is the sampling frequency which is 0.1 ms in the experimental set up. Since the pole of digital delay compared with the DFIG plant is too small, it can be simplified as 1. Thus, proportional and integral gain of rotor current control loop can be calculated as,

$$k_{pc} = 100\times 2\pi\times\sigma L_r = 6.9,\ k_{ic} = 100\times 2\pi\times R_r = 553 \tag{14}$$

The rotor current control loop can be simplified as an inertia block. Combining (12) and (13), the block diagram of stator power and frequency control loop can be shown in Fig. 5.

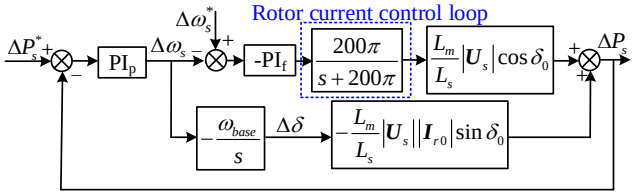

Fig. 5. Block diagram of stator power and frequency control loop.

In order to reduce the system order, the parameters of the stator frequency PI controller is designed to counteract the pole rotor current loop, and the bandwidth of the frequency control loop is designed as 20 Hz. Thus, the proportional and integral gain of stator frequency PI controller can be calculated as,

$$k_{pf} = 40\pi/200\pi = 0.2,\ k_{if} = 1\times 40\pi = 126 \tag{15}$$

In order to simplify the power control loop, the operation point near zero output power is chosen to design the parameter. In this way, the angle δ_0 is almost 90 °, $\cos\delta_0$ is equal to zero and $\sin\delta_0$ is equal to 1. Thus, the power control loop can be simplified as shown in Fig. 6.

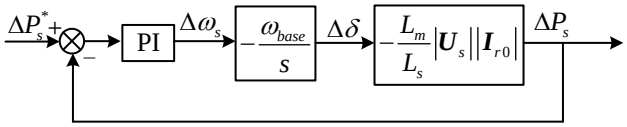

Fig. 6 Block diagram of simplified power control loop

The closed loop transfer function of power loop can be deduced as,

$$\frac{\Delta P_s}{\Delta P_s^*} = \frac{ak_{ip}}{s^2 + ak_{pp}s + ak_{ip}} = \frac{\omega_n^2}{s^2 + 2\xi\omega_n s + \omega_n^2} \tag{16}$$

where $a = L_m/L_s\cdot\omega_{base}|\boldsymbol{U}_s||\boldsymbol{I}_{r0}|$. As can be seen from the transfer function of power loop, it is a second order system. According to the design principle of second order system, the damping ratio ξ is always set as 0.707 and the natural frequency is designed based on the dynamic performance requirement. In this letter, the bandwidth of the outer power control is designed as 10 Hz. Thus, the ω_n is set as 20π rad/s. The proportional and integral parameters can be obtained as,

$$k_{pp} = 2\xi\omega_n/a = 0.69,\ k_{ip} = \omega_n^2/a = 30 \tag{17}$$

According to Fig. 5, the characteristic equation of the stator power and stator frequency control system can be deduced as,

$$G_{cha} = 1 + \frac{L_m|\boldsymbol{U}_s|}{L_s}\frac{k_{pp}s + k_{ip}}{s}\left(\frac{40\pi}{s+40\pi}\cos\delta_0 + \frac{\omega_{base}}{s}|\boldsymbol{I}_{r0}|\sin\delta_0\right) \tag{18}$$

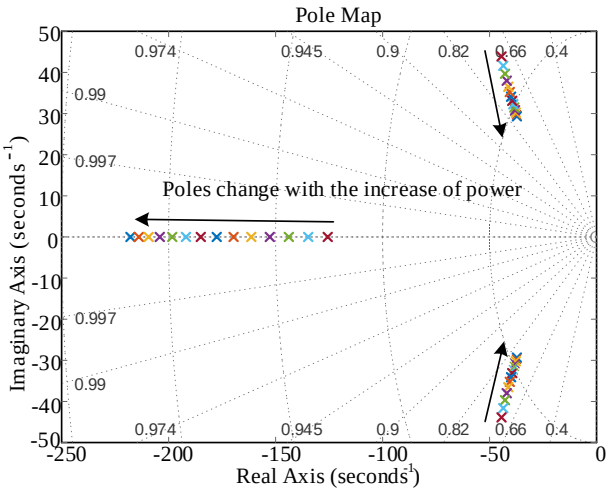

Fig. 7. Pole map with stator power changing from 0 to 1 pu.

According to the characteristic equation shown in (18), the pole map of stator power changing from zero to 1 pu is plotted in Fig. 7. The system has three poles，one negative real pole and two conjugate poles. All the poles are located in the left half

This article has been accepted for publication in a future issue of this journal, but has not been fully edited. Content may change prior to final publication. Citation information: DOI 10.1109/TIE.2019.2956415, IEEE Transactions on Industrial Electronics

plane which indicates that the power and stator frequency control loops are always stable. When the stator power is zero, the power control loop is still effective. However, it should be noted that the stator frequency control loop can not work in the zero power mode since the equation (1) is not satisfied under this condition. In that way, the stator frequency can not be controlled by the magnitude of stator flux. In the zero output power mode, the system will stop working or will change to an open loop mode which will just directly use a given transformation angle. The zero power mode has been elaborated in [4], which is not repeated in this letter.

V. Experimental Results

In order to validate the rotor current oriented control method, a DFIG-based experimental system shown as Fig. 1 is developed. The control strategy of RSC is implemented on the TI TMS320F28335 DSP and the switching frequency is 10 kHz with a sampling frequency of 10 kHz. The parameters of the DFIG are shown in Table 1. All the waveforms are acquired by a YOKOGAWA DL750 scope.

TABLE I Parameters of the tested DFIG-DC system

Parameters	*Value*	*Parameters*	*Value*
Rated power	1.0 kW	Rated voltage	110 V
Rated frequency	50 Hz	DC voltage	140 V
Stator/rotor	0.33	R_s	1.01 Ω
R_r	0.88 Ω	L_m	87.5 mH
$L_{\sigma s}$	5.6 mH	$L_{\sigma r}$	5.6 mH

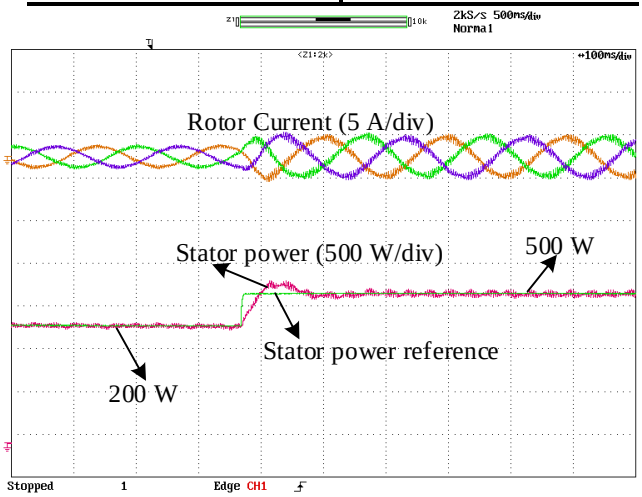

Fig. 8. Step response of stator power change.

Fig. 8 shows a step response of DFIG when the stator active power reference changes from 200 W to 500 W. The rotor speed is 900 rpm and the stator frequency is set as 50 Hz. The stator active power has a little overshoot but can track the power reference accurately in 110 ms without any steady state error, which corresponds with the small signal model and the parameter design in section IV.

The step response of the stator frequency changing from 55 Hz to 50 Hz is shown in Fig. 9. The stator power reference is 400 W. During the change of stator frequency, the stator power has a pulsation which is caused by transient stator flux but will come to steady state in 80 ms. The stator frequency can quickly track the reference frequency in 60 ms without any overshoot which validates the effectiveness of stator frequency control loop.

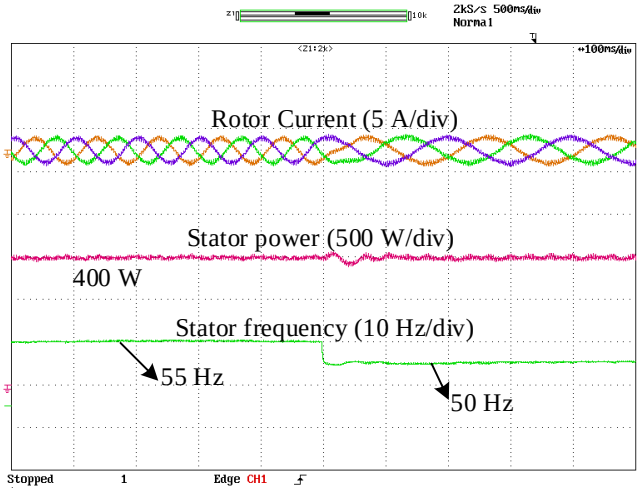

Fig. 9. Step response of stator frequency change.

VI. Conclusion

This letter proposes an enhanced stator frequency and power control method of DFIG-DC system based on rotor current orientation. The stator power is controlled by the angle of rotor current vector and the stator frequency is controlled by the magnitude of rotor current. Since only the rotor current is necessary for the control, the stator voltage sensors and current sensors can be avoided. Furthermore, the effectiveness of stator power and frequency control loop are verified by small signal analysis and also experimental results.

References

[1] N. Yu, H. Nian, and Y. Quan, "A novel DC grid connected DFIG system with active filter based on predictive current control," in *Proc. Int. Conf. Elect. Mach. Syst.*, Aug. 22–23, 2011, pp. 4525–4537

[2] H. Nian and X. Yi, "Coordinated control strategy for doubly-fed induction generator with dc connection topology," *IET Renew. Power Gener.*, vol. 9, no. 7, pp. 747–756, Aug. 2015.

[3] M. F. Iacchetti, G. D. Marques, R. Perini, "Operation and design issues of a DFIG stator-connected to a DC-net by a diode rectifier," *IET Electric Power Applications*, vol 8, no. 8, pp. 310-319, Sep. 2014.

[4] G. D. Marques, M. F. Iacchetti, "Stator frequency regulation in a field oriented controlled DFIG connected to a DC link," *IEEE Trans. Ind. Electron.*, vol. 61, no. 11, pp. 5930-5939, Nov. 2014.

[5] G. D. Marques, M. F. Iacchetti, "Inner control method and frequency regulation of a DFIG connected to a DC link," *IEEE Trans. Energy convers.*, vol.29, no.2, pp.435-444, Jun. 2014.

[6] M. F. Iacchetti, G. D. Marques, and R. Perini, "Torque ripple reduction in a DFIG-DC system by resonant current controllers," *IEEE Trans. Power Electron.*, vol. 30, no. 8, pp. 4244–4254, Aug. 2015.

[7] H. Nian, C. Wu, and P. Cheng, "Direct resonant control strategy for torque ripple mitigation of DFIG connected to DC link through diode rectifier on stator," *IEEE Trans. Power Electron.*, vol. 32, no. 9, pp. 6936–6945, Sep. 2017.

[8] G. D. Marques, M. F. Iacchetti, "A self-sensing stator-current-based control system of a DFIG connected to a DC-link", *IEEE Trans. on Power Electron.*, vol. 62, no. 10, pp. 6140-6150, Oct. 2015.

[9] C. Wu and H. Nian, "Sinusoidal current operation of DFIG-DC System without stator voltage sensors," *IEEE Trans. Ind. Electron.*, vol. 65, no. 8, pp. 6250–6258, Aug. 2018

[10] C. Wu, H. Nian, "An improved repetitive control of DFIG-DC system for torque ripple suppression," *IEEE Trans. on Power Electron.*, vol. 33, no.9, pp. 7634-7644, Sep. 2018.
[11] H. Misra and A. K. Jain, "Analysis of stand alone DFIG-DC system and DC voltage regulation with reduced sensors," *IEEE Trans Ind. Electron.*, vol. 64, no. 6, pp. 4402–4412, Jun. 2017.
[12] D. Zhou, F. Blaabjerg. "Bandwidth oriented proportional-integral controller design for back-to-back power converters in DFIG wind turbine system," *IET Renew. Power Gener.*, vol. 11 no. 7, pp. 941-951, 2017.